AMERICAN SOCIETY FOR MICROBIOLOGY | Journal of Virology®

The Major Envelope Glycoprotein of Murid Herpesvirus 4 Promotes Sexual Transmission

Caroline Zeippen,[a] Justine Javaux,[a] Xue Xiao,[a] Marina Ledecq,[b] Jan Mast,[b] Frédéric Farnir,[c] Alain Vanderplasschen,[a] Philip Stevenson,[d] Laurent Gillet[a]

Immunology-Vaccinology, Department of Infectious and Parasitic Diseases, Faculty of Veterinary Medicine-Fundamental and Applied Research for Animals and Health (FARAH), University of Liège, Liège, Belgium[a]; Electron Microscopy Unit, Veterinary and Agrochemical Research Centre (CODA-CERVA), Uccle, Belgium[b]; Biostatistics and Bioinformatics Applied to Veterinary Science, Department of Animal Productions, Faculty of Veterinary Medicine-FARAH, University of Liège, Liège, Belgium[c]; School of Chemistry and Molecular Biosciences, University of Queensland and Royal Children's Research Hospital, Brisbane, Queensland, Australia[d]

ABSTRACT Gammaherpesviruses are important human and animal pathogens. Infection control has proven difficult because the key process of transmission is ill understood. Murid herpesvirus 4 (MuHV-4), a gammaherpesvirus of mice, is transmitted sexually. We show that this depends on the major virion envelope glycoprotein gp150. gp150 is redundant for host entry, and *in vitro*, it regulates rather than promotes cell binding. We show that gp150-deficient MuHV-4 reaches and replicates normally in the female genital tract after nasal infection but is poorly released from vaginal epithelial cells and fails to pass from the female to the male genital tract during sexual contact. Thus, we show that the regulation of virion binding is a key component of spontaneous gammaherpesvirus transmission.

IMPORTANCE Gammaherpesviruses are responsible for many important diseases in both animals and humans. Some important aspects of their life cycle are still poorly understood. Key among these is viral transmission. Here we show that the major envelope glycoprotein of murid herpesvirus 4 functions not in entry or dissemination but in virion release to allow sexual transmission to new hosts.

KEYWORDS gammaherpesvirus, glycoprotein, release, transmission

Received 10 February 2017 **Accepted** 10 April 2017

Accepted manuscript posted online 19 April 2017

Citation Zeippen C, Javaux J, Xiao X, Ledecq M, Mast J, Farnir F, Vanderplasschen A, Stevenson P, Gillet L. 2017. The major envelope glycoprotein of murid herpesvirus 4 promotes sexual transmission. J Virol 91:e00235-17. https://doi.org/10.1128/JVI.00235-17.

Editor Richard M. Longnecker, Northwestern University

Address correspondence to Laurent Gillet, L.Gillet@ulg.ac.be.

Transmission is the main motor of viral evolution, and the large disease burden imposed by human gammaherpesviruses reflects very high infection prevalences due to efficient transmission from carriers to new hosts (1). Epstein-Barr virus (EBV) and Kaposi's sarcoma-associated herpesvirus (KSHV) infect up to 90% (2) and 30% (3) of humans worldwide, respectively. Endemic infections are maintained chiefly by carriers shedding virus in their saliva. However, in populations with a low prevalence of infection, sexual transmission becomes important due to increased contact (4). This was seen clearly for KSHV transmission associated with HIV infection (5) and may also apply to EBV (6).

While interrupting transmission is the *sine qua non* of infection control, analyzing EBV and KSHV transmission has proven difficult. Natural EBV infection is asymptomatic for at least a month (6), and experimental transmission is made difficult by many EBV and KSHV functions being host specific. However, gammaherpesviruses colonize most mammals, so related animal viruses, such as murid gammaherpesvirus 4 (MuHV-4), provide another way to understand infection *in vivo* (7). Luciferase (Luc) imaging of MuHV-4 infection (8) revealed genital infection following intranasal (i.n.) inoculation of female mice, which then spread to naive males by sexual contact (9). This has provided

a basis for understanding the molecular determinants of gammaherpesvirus transmission.

Virion glycoproteins are likely the main actors in transmission. The MuHV-4 envelope displays at least 10 membrane-bound proteins (10, 11). gH, gB, gM, and gN are essential for infectivity, while gL, gp70, gp150, open reading frame 58 (ORF58), ORF27, and ORF28 are redundant. ORF28 has no known function (12). ORF27 and ORF58 form a complex involved in direct cell-to-cell viral spread (13). gM/gN is probably required for virion assembly (14). gp70, gH/gL, and gB all contribute to cell binding and/or entry (15, 16). A surprising finding was that gp150, the MuHV-4 equivalent of gp350/220 in EBV (17), K8.1A in KSHV (18), and gp180 in bovine gammaherpesvirus 4 (BoHV-4) (19), is redundant for both cell binding *in vitro* and virion entry into naive hosts (20). Moreover, gp150-deficient virions show enhanced binding to cells that express little heparan (20).

Heparan binding is a key event in infection by cell-free MuHV-4 (21), a characteristic shared by many herpesviruses. MuHV-4 binds to heparan via gH/gL and by gp70 (15, 16). While heparan is abundant on most transformed stromal cells, the apical surfaces of most differentiated epithelia display much less heparan. However, the lungs and olfactory epithelium, which are efficiently targeted by MuHV-4, display heparan. Specifically, nonsulfated heparan, which is bound by gH/gL, is present on the apical cilia of olfactory neurons (22) and on type 1 alveolar epithelial cells (23). The genital tract is not known to express apical heparan, and here host entry may depend on sexual contact causing epithelial trauma, which exposes the abundant heparan of basolateral epithelial surfaces (24).

MuHV-4 also binds to nonheparan ligands, for example, via gB (25), but this binding appears not to be available until heparan is engaged. Thus, the dependence of virions on heparan reflects both positive and negative regulation. Negative regulation is mediated by gp150, suggesting that heparan displaces it from covering an important non-heparan binding site (26). The main *in vitro* defect of gp150-deficient (gp150$^-$) MuHV-4 is poor release from infected cells, which tend to lose heparan and are probably coated by the abundantly shed heparan binding domains of gp70 (15, 20). gp150 itself binds heparan only weakly, but heparan and gp150 are presumably brought into close contact by the strong interactions of gH/gL and gp70. BoHV-4 gp180 also binds to heparan and regulates heparan-independent virion-cell binding (19). KSHV K8.1 binds to heparan, and there have been suggestions of a regulatory role (27, 28). EBV gp350 does not bind to heparan (this is a function of EBV gp150 [29]). However, gp350 regulates binding to epithelial cells (30), suggesting that it promotes virion release from epithelial cells. Thus, the regulation of cell binding by the major envelope glycoprotein is a common gammaherpesviruses theme.

Despite the importance of gp150 for MuHV-4 release from infected cells, gp150-deficient mutants show no defect in host colonization after nasal inoculation (20, 31). This reflects that host colonization is driven primarily by lymphoproliferation and cell-cell virus transfer (32). The main function of cell-free virions is viral genome transfer to new hosts. Standard pathogenesis models ignore this crucial component of the viral life cycle. Here we show that gp150-deficient MuHV-4 has no defect in genital tract colonization but transmits poorly to new hosts. This reflected poor virion release from the female vaginal epithelium.

RESULTS

Generation of luciferase-positive gp150$^-$ MuHV-4. Viral luciferase expression is a key tool for monitoring infection *in vivo* (8). Thus, to track infection by gp150$^-$ MuHV-4, we generated a luciferase-positive (Luc$^+$) version of the previously studied M7-STOP mutant (20) (Fig. 1A). The predicted genomic structure was confirmed by restriction enzyme digestion and Southern blotting of viral DNA (Fig. 1B). Genome sequencing confirmed a lack of mutations elsewhere (data not shown). Analysis of infected cells confirmed a lack of gp150 expression by gp150$^-$ Luc MuHV-4 (Fig. 1C), while the expressions of other glycoproteins were similar.

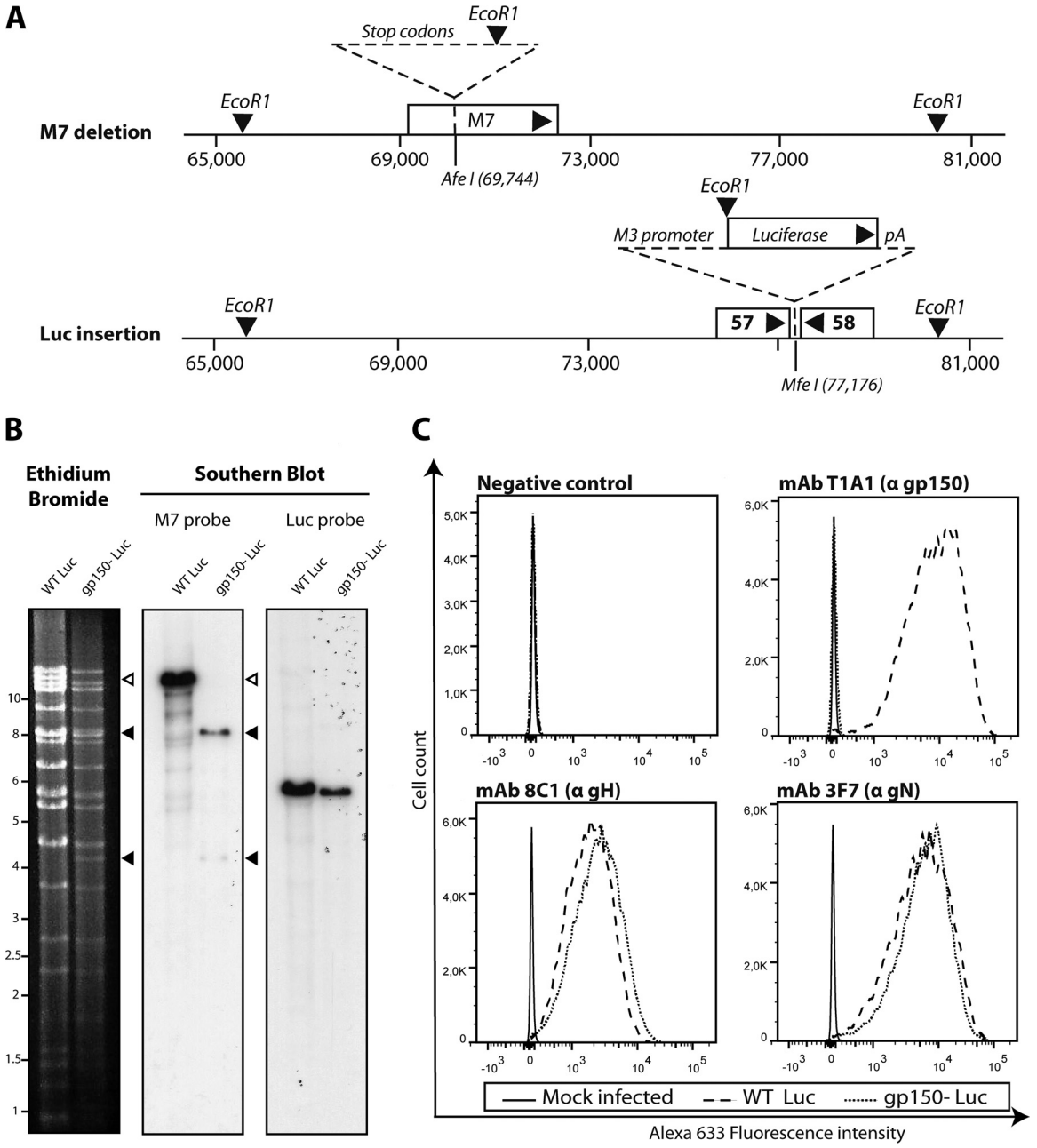

FIG 1 Generation of gp150$^-$ MuHV-4 expressing luciferase. (A) Two tested MuHV-4 mutations were combined. To disrupt gp150, stop codons and an EcoRI restriction site were inserted into an AfeI site at genomic position 69473 (20). To express luciferase, an M3 promoter-driven cassette was inserted into the MfeI site at genomic position 77176 (8). (B) Viral DNA was digested with EcoRI, resolved by agarose gel electrophoresis, and hybridized with ^{32}P-labeled probes, corresponding to nucleotides 69467 to 70918 (M7 open reading frame) of MuHV-4 and to the firefly luciferase coding sequence (pGL4.10; Promega). The open arrow shows the WT M7 fragment (13,724 bp). Black arrows show the restriction fragments containing M7-STOP. (C) Mutants were analyzed for infected-cell glycoprotein expression by flow cytometry. We used monoclonal antibodies recognizing gp150 (T1A1), gH (8C1), and gN (3F7) (14, 15, 47).

gp150$^-$ MuHV-4 shows no infection defect after intranasal inoculation. Female BALB/c mice ($n = 20$) were given wild-type (WT) or gp150$^-$ Luc MuHV-4 i.n., and infection was tracked by using an *in vivo* imaging system (IVIS) (Fig. 2A). A luminescent signal was observed in the nose and thoracic region at day 7 postinfection (p.i.) and in the neck and left abdominal region at day 14 p.i. (Fig. 2B and C). These signals correspond to lytic infection in the nose, lungs, superficial cervical lymph nodes (SCLN), and spleen (8). gp150$^-$ MuHV-4 showed greater SCLN signals ($P < 0.01$), but otherwise, there was no difference between infection groups.

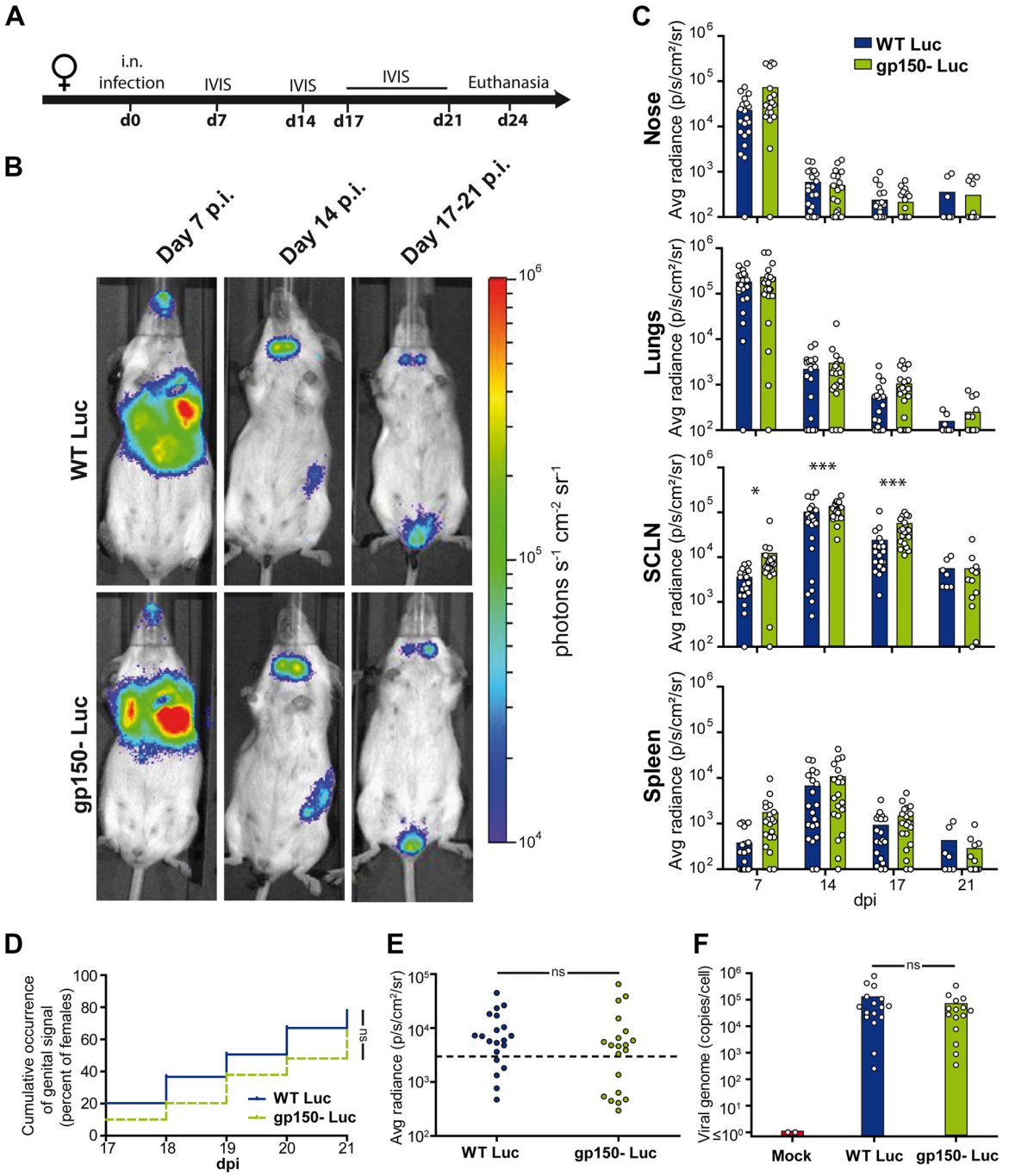

FIG 2 Bioluminescence imaging of gp150$^-$ MuHV-4. (A) Female mice were infected intranasally with gp150$^+$ or gp150$^-$ Luc MuHV-4 (10^4 PFU under general anesthesia) and imaged at the times indicated. (B) Representative images are shown for each group at days 7, 14, and 17 to 21 p.i. (C) Signal intensities were compared for each organ ($n = 20$ mice per group), measuring equivalent regions of interest and subtracting the right abdominal signal as a negative background. The limit of detection of the assay is 10^2 photons/s/cm^2/sr. Results were analyzed by a linear model, using day postinfection, strain, and interaction between day and strain as factors ($P > 0.05$ for all comparisons, except for the SCLN, where gp150$^-$ signals were significantly higher at days 7, 14, and 17 [*, $P < 0.05$; ***, $P < 0.001$]). (D and E) To assay genital tract colonization, mice were imaged every day from days 17 to 21 p.i. Positive signals were taken as those >2 standard deviations above the mean for 10 uninfected mice (threshold represented by the dashed line). The occurrence of a genital signal (D) ($n = 40$ mice per group) and the maximal genital signal (E) ($n = 20$ mice per group) showed no significant difference between groups ($P > 0.05$ by chi-square and Mann-Whitney tests, respectively). (F) The smallest pieces of genital tissue expressing luciferase were isolated. Genome copy numbers were then measured by qPCR and did not show a significant difference between groups ($n = 20$ mice per group; $P > 0.05$ by a Mann-Whitney test). The histograms show mean values. The results are representative of data from three independent experiments. ns, not significant.

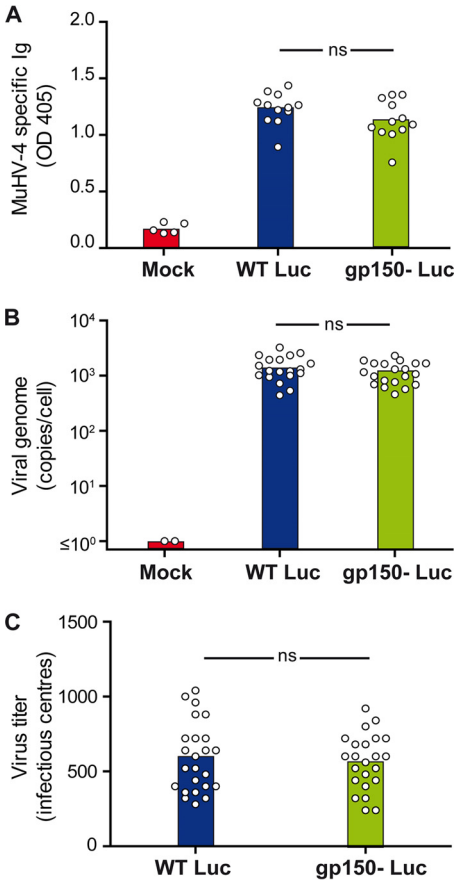

FIG 3 Seroconversion and latency establishment after intranasal inoculation of gp150$^+$ and gp150$^-$ MuHV-4. Female mice were infected intranasally with WT or gp150$^-$ MuHV-4 (10^4 PFU under general anesthesia). At 1 month p.i., sera and spleen were collected. (A) ELISA of sera shows no difference in MuHV-4-specific antibodies between groups ($P > 0.05$ by one-way analysis of variance and a Bonferroni *post hoc* test). OD 405, optical density at 405 nm. (B and C) Viral genome copy numbers in spleen measured by qPCR show no significant difference between groups ($P > 0.05$ by one-way analysis of variance and a Bonferroni *post hoc* test) (B), nor did infectious center assays of spleens show a difference between groups ($P > 0.05$ by the Student test) (C). Mean values are represented by histograms.

Between days 17 and 21 p.i., the mice were imaged daily to observe the transient genital signal (9). By this time, primary lytic infection had resolved, and the luciferase signals from lymphoid organs were greatly reduced compared with those at day 14. Genital luciferase signals were detectable in 77% of mice given gp150-positive (gp150$^+$) MuHV-4 and in 64% of those given gp150$^-$ MuHV-4 ($P > 0.05$) (Fig. 2D). The maximum intensity of the genital signal showed no difference between groups ($P > 0.05$) (Fig. 2E), nor did the viral DNA loads of luciferase-positive vaginal mucosa samples (Fig. 2F). Thus, gp150$^-$ MuHV-4 showed no defect in genital colonization after i.n. inoculation.

At 1 month p.i., sera were assayed for MuHV-4-specific IgG by an enzyme-linked immunosorbent assay (ELISA) (Fig. 3A). No difference between gp150$^+$ and gp150$^-$ infections was observed ($P > 0.05$). At the same time, quantitative PCR (qPCR) of spleen DNA showed no difference in viral genome loads between gp150$^+$ and gp150$^-$ MuHV-4 (Fig. 3B and C). Thus, gp150$^-$ MuHV-4 showed no defect in the extent of infection or the capacity to establish latency in the spleen.

gp150 promotes sexual transmission from female to male after intranasal infection. To assay transmission, intranasally infected female BALB/c mice were mated with BALB/c males at the time of the appearance of a genital signal (between days 17 and 21 p.i.), mixing 3 naive males with 3 excreting females (Fig. 4A). In total, in 2 independent experiments, 34 males were mated with gp150$^+$ MuHV-4-infected fe-

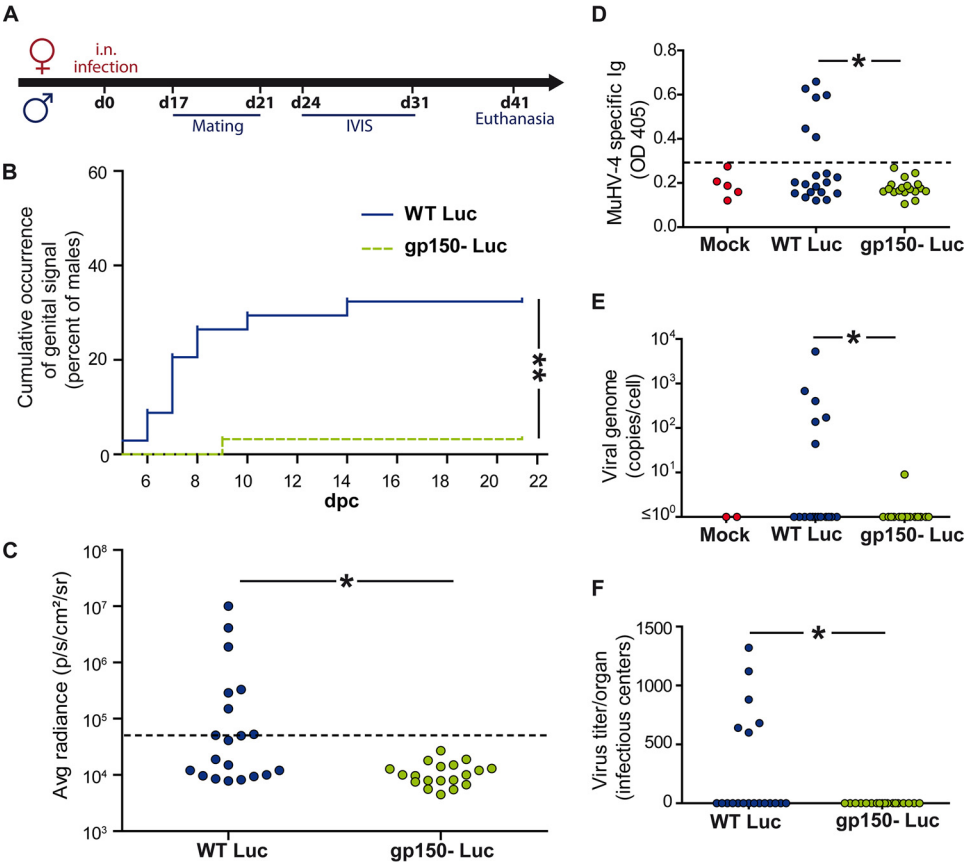

FIG 4 gp150 promotes MuHV-4 sexual transmission. Female BALB/c mice were infected intranasally with gp150$^+$ or gp150$^-$ MuHV-4 (10^4 PFU under general anesthesia) and imaged at the indicated times. When a genital signal appeared, female mice were mated with naive BALB/c males, which were then monitored in turn by an IVIS. (A) Experimental scheme. (B and C) Occurrence of positive genital signals (B) and maximal genital signals (C) in males, imaged between 3 and 21 days after contact with females. Signal intensities were measured in equivalent regions of interest, subtracting the right abdominal region as the background. Males with a genital signal >2 standard deviations above the mean for 10 controls (the dotted line in panel C) were considered positive ($n = 6$ in panel C; $P < 0.05$ by a Fisher test). Panel B shows pooled data for 2 experiments ($P < 0.01$ by a Fisher test). Panel C shows 1 experiment (20 mice per group). (D to F) Male infections were confirmed at 1 month by an ELISA of serum for MuHV-4-specific Ig (D), qPCR of splenic viral genome loads (E), and an infectious center assay of spleens (F). dpc, days postcontact. Panels D to F all show significant differences by a Fisher test ($P < 0.05$).

males, and 30 males were mated with gp150$^-$ MuHV-4-infected females. Males were imaged every 3 to 4 days over 3 weeks. A total of 32% of males ($n = 11$) in the gp150$^+$ group and 3% of males ($n = 1$) in the gp150$^-$ group showed a genital signal (Fig. 4B). Figure 4C shows the maximal male genital signals measured at between days 7 and 17 postcontact in 1 experiment.

At 1 month postcontact, serum and spleen were collected from males to confirm the results of *in vivo* imaging. MuHV-4-specific antibodies were detected in all the males that had positive IVIS signals (Fig. 4D shows data from 1 experiment). The same animals were also positive for splenic viral DNA by quantitative PCR and for reactivatable splenic virus by an infectious center assay (Fig. 4E and F). Thus, gp150$^-$ MuHV-4 showed significantly less female-to-male transmission than did gp150$^+$ MuHV-4.

gp150 does not promote infection of the penile mucosa. We considered that gp150 disruption might reduce transmission by reducing virus entry into the male penile mucosa. To test this hypothesis, 30 males were anesthetized with isoflurane, and gp150$^+$ or gp150$^-$ MuHV-4 (10^5 PFU in 15 μl phosphate-buffered saline [PBS]) was put into contact with scraped penile mucosa for 20 min. IVIS imaging over the next 8 days showed 11/15 infected males in each group (Fig. 5). Thus, gp150 was not required to infect the penile mucosa.

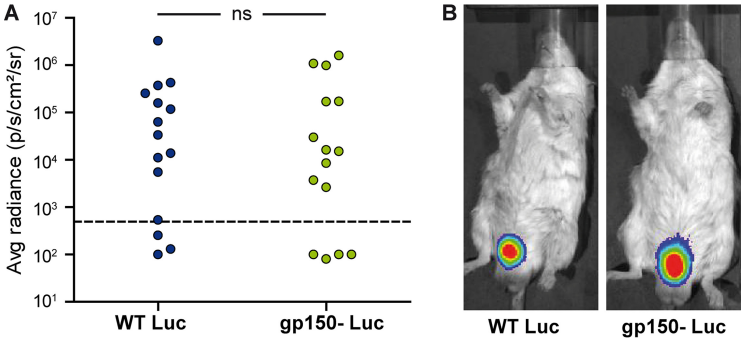

FIG 5 MuHV-4 infection of male genital mucosa. Male BALB/c mice ($n = 15$ per group) were infected under general anesthesia by scraping virions (10^5 PFU) onto the penile mucosa. Animals were imaged for eight consecutive days. (A) Maximal genital signal observed for each male by *in vivo* imaging at between days 1 and 8 p.i. ($P > 0.05$ by a Fisher test). (B) Images showing a representative positive mouse from each group.

gp150 does not promote transmission by protecting against neutralization. gp150 is an immunodominant glycoprotein and, as anti-gp150 antibodies are nonneutralizing, helps by its immunogenicity to protect virions against neutralization (33). gp150-specific antibodies additionally promote MuHV-4 entry into IgG Fc receptor-positive cells, and its gp180 homolog in BoHV-4 acts as a protective glycan shield (34). Thus, although MuHV-4-specific antibody responses are relatively weak at 1 month postinfection (35), gp150 could potentially promote transmission by reducing the impact of antibodies. To test this hypothesis, we first looked for MuHV-4-specific antibodies in vaginal secretions (Fig. 6A). These antibodies were present at low titers in a minority of infected mice, with no significant difference between the 2 groups ($P > 0.05$). We also tested the susceptibility of gp150$^+$ and gp150$^-$ virions to neutralization by sera of mice infected by the same virus for 1 month (Fig. 6B). No significant difference was observed ($P > 0.05$), except at one dilution of serum where gp150$^+$ virions were significantly more neutralized by the homologous serum ($P < 0.01$). Thus, gp150 seemed not to promote transmission by directly protecting vulnerable epitopes against antibody neutralization.

gp150 promotes the release of infectious MuHV-4 virions from vaginal mucosa. gp150 promotes virion release from infected cells *in vitro* (20). Thus, we considered that gp150$^-$ Luc virions might be poorly released into vaginal secretions and thus be less

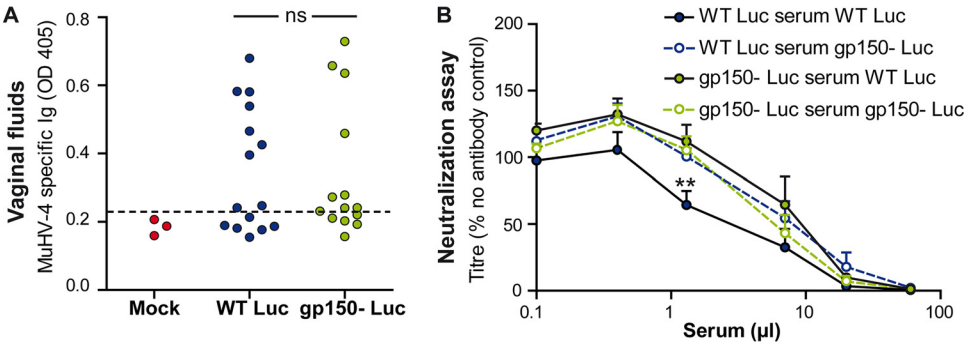

FIG 6 Importance of gp150 for protection against neutralizing antibodies. (A) Female BALB/c mice were infected intranasally with gp150$^+$ or gp150$^-$ MuHV-4 (10^4 PFU under general anesthesia), and vaginal fluids collected at day 24 p.i. were tested by an ELISA for MuHV-4-specific antibodies. No difference was observed between groups ($P > 0.05$ by a Fisher test). (B) gp150$^+$ and gp150$^-$ virions (200 PFU) were incubated (1 h at 37°C) with dilutions of sera from BALB/c mice infected with the same viruses 1 month previously. After incubation, the virus-serum mixtures were plaque assayed on BHK-21 cells. Titers are expressed relative to values for virus without an antibody. The data show averages of data from triplicate measurements ± standard errors of the means and were analyzed by two-way analysis of variance and Bonferroni *post hoc* tests. No significant difference was observed ($P > 0.05$), except at one dilution of serum, where gp150$^+$ virions were significantly more neutralized by gp150$^+$ MuHV-4-elicited antibody (**, $P < 0.01$).

available for penile infection. To test this hypothesis, female BALB/c mice were infected intranasally, and when genital luciferase signals were observed, vaginal washouts were collected for a plaque assay. To distinguish cell-free from cell-associated virions, the vaginal washouts were centrifuged at 100 × *g* (10 min) to collect cell-associated virions and then at 20,000 × *g* (90 min) to collect cell-free virions. The infection groups showed no significant difference in cell-associated infectivity ($P > 0.05$), but a lack of gp150 significantly reduced cell-free infectivity ($P < 0.05$) (Fig. 7A). We also compared gp150$^+$ and gp150$^-$ virus growth in primary vaginal epithelial cells. While levels of gp150$^+$ virions were split equally between the supernatants and cells at 24 h p.i. and then progressively increased in the supernatants, gp150$^-$ virions were strongly cell associated (Fig. 7B).

Data from staining of infected cells for gN (Fig. 7C) supported the idea of virion retention: staining of fixed-permeabilized cells showed no significant difference between gp150$^+$ and gp150$^-$ MuHV-4 ($P > 0.05$), indicating similar infections, but staining of nonpermeabilized cells showed significantly more cell surface gN after gp150$^-$ MuHV-4 infection ($P < 0.001$) (Fig. 7C and D). Besides increased virus retention at the cell surface, increased gN detection could also be consecutive to increased gN cell surface expression in cells infected with gp150-deficient virus or to increased epitope access in the absence of gp150. To distinguish between these hypotheses by direct visualization, we performed transmission electronic microscopy (TEM) of infected vaginal cells. The cells were exposed to gp150$^+$ or gp150$^-$ MuHV-4 (1 PFU/cell) and then analyzed by TEM 24 h and 48 h later. gp150$^+$ virions never formed more than a single layer at the infected cell surface. In contrast, gp150-deficient virions formed multiple layers (Fig. 7E). Such aggregates were not observed in viral stocks, showing that virions do not spontaneously aggregate with each other (data not shown). Thus, gp150$^-$ virions were poorly released from vaginal epithelial cells.

DISCUSSION

Viral transmission is a crucial determinant of disease burden. For example, spikes in diseases caused by Ebola and avian influenza viruses are associated with increased infection rates rather than more virulent infections (36, 37). Conversely, while both live and killed poliovirus vaccines prevent disease, eradication has depended on live vaccines because it more effectively inhibits transmission (38). For herpesviruses, which are highly prevalent and only sometimes cause disease, transmission is a key intervention target. However, even established live-attenuated vaccines that prevent disease are probably insufficient by themselves to prevent transmission (39). Therefore, it is important to understand this process better.

Herpesvirus transmission has proven difficult to replicate in experimental settings and is ignored by most standard pathogenesis assays of host colonization/disease after deliberate inoculation. Murine cytomegalovirus is transmitted via the upper respiratory tract (40). MuHV-4 also enters new hosts via the upper respiratory tract (22). However, it has not been shown to be transmitted spontaneously by this route. This may reflect that most experimental settings favor low-frequency/high-penetrance contacts, rather than the high-frequency/low-penetrance contacts of natural, endemic virus exchange. Nonetheless, sexual contact may be a significant mode of transmission for many herpesviruses in populations with a low prevalence of infection (4), as observed for KSHV (5) and potentially EBV (6). gp150 provides the first example of a viral glycoprotein important for transmission but not for entry or dissemination, because it is important for virion release.

Escape from infected cells poses a general problem for nonmotile pathogens. One solution is to produce large numbers of infectious particles and cause widespread epithelial destruction. The *modus operandi* of herpesviruses, which are transmitted chronically, at a low level, and for the most part without symptoms, seems instead to center on entry and exit at different sites, for example, entry at the olfactory epithelium, where there is apical heparan, and exit from the oropharynx, where heparan is basolateral (22). Sexual transmission seems to go against this paradigm, as entry and

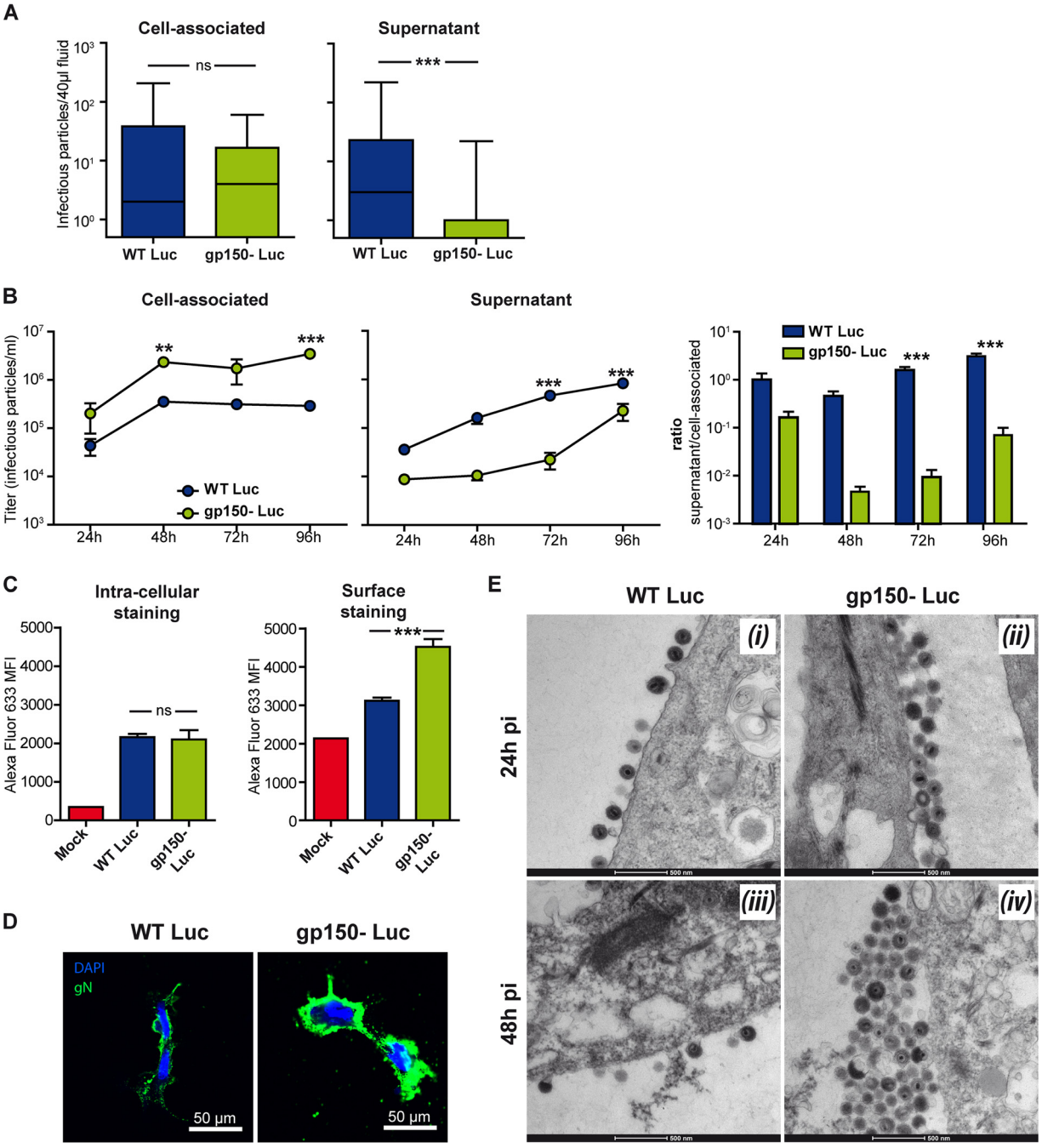

FIG 7 Defective gp150 virion release from vaginal epithelial cells. (A) Female BALB/c mice were infected intranasally with gp150$^+$ or gp150$^-$ MuHV-4 (10^4 PFU under general anesthesia) and serially imaged by an IVIS. When a genital signal appeared, vaginal fluids were collected by lavage. Cell-associated and cell-free virions were separated by successive centrifugations. Each virion type was quantified by a plaque assay. Results were analyzed by a Mann-Whitney test (ns, not significant [$P > 0.05$]; ***, $P < 0.001$). (B) Primary vaginal epithelial cells were infected with gp150$^-$ or gp150$^+$ MuHV-4 (0.05 PFU/cell). Supernatants and cells were collected and plaque assayed on BHK-21 cells. Results were analyzed by two-way analysis of variance and Bonferroni *post hoc* tests (**, $P < 0.01$; ***, $P < 0.001$). (C) Primary vaginal epithelial cells were infected with gp150$^-$ or gp150$^+$ MuHV-4 (1 PFU/cell for 18 h) and then stained for gN. Staining of fixed and permeabilized cells was used to assess total infection, while staining of intact cells was used to estimate virion numbers at the cell surface. (gM/gN homes strongly to the Golgi network and thus reaches the cell surface only by virtue of incorporation into virions [14].) Mean fluorescence intensities (MFI) were analyzed by one-way analysis of variance and Bonferroni *post hoc* tests (ns, $P > 0.05$; ***, $P < 0.001$). These results are representative of data from at least 3 experiments. (D) Primary vaginal cells were infected with gp150$^+$ or gp150$^-$ MuHV-4 (2 PFU/cell). At 48 h p.i., cells were stained for gN, counterstained with 4′,6-diamidino-2-phenylindole (DAPI), and observed by confocal microscopy. (E) Primary vaginal cells were infected with gp150$^+$ or gp150$^-$ MuHV-4 (1 PFU/cell) and then processed for TEM. The pictures are representative of results from at least 10 sections per sample: panels i and ii are from 24 h p.i., and panels iii and iv are from 48 h p.i.

exit then overlap. For MuHV-4, the lack of its key binding target, heparan, on the apical genital epithelium (41) suggests that tissue trauma is required for host entry. With sexual transmission, this is entirely plausible. Barring too much tissue trauma in the virus donor, genital epithelia should then efficiently shed heparan-dependent virions. Indeed, during sexual transmission, shedding probably precedes trauma. Accordingly, a loss of heparan dependence through gp150 disruption severely compromised MuHV-4 shedding and subsequent virus transmission. In the absence of gp150, the newly produced virions likely bind to components present at the cell surface. Thus, the unknown cell ligand for which gp150 regulates binding could be cleaved or have a secreted form that could cause virion aggregation and poor release. The nature of this cellular component will have to be investigated in the future. Thus, heparan dependence is not just a means of virion capture but a switch that enables both virion capture and release to be efficient. We envisage that BoHV-4 gp180, KSHV K8.1A, and EBV gp350 also promote transmission by virion release, at both genital and oral mucosal surfaces, in addition to any roles that they have in host entry.

Could virus shedding be targeted by vaccination? We believe that this is unlikely to be achieved by targeting gp150 or its homologs, as they are already highly immunogenic in virus carriers (33). gp150-specific antibodies fail to neutralize MuHV-4; their main effect is to increase infection of cells with low levels of heparan and high levels of IgG Fc receptors (38), while (monoclonal) antibodies to EBV gp350 promote epithelial infection (42). In contrast, shedding of infectious virus could potentially be reduced by boosting other, subdominant antibody specificities in virus carriers (43). This remains to be tested in the transmission model. The feasibility of this approach is also supported by the fact that gp150 likely does not act as a glycan shield (Fig. 6B), in contrast to its homolog in BoHV-4 (34).

Altogether, the present study identifies for the first time the importance of a specific gammaherpesvirus glycoprotein in transmission. gp150 did this by promoting virion release from infected vaginal epithelial cells. These results establish a new and important gp150 function that may well also apply to its homologs in human pathogens.

MATERIALS AND METHODS

Animals. BALB/c mice were housed at the University of Liège, Department of Infectious Diseases, FARAH. The Committee on the Ethics of Animal Experiments of the University of Liège approved the protocol (permit number 1502).

Female mice were infected intranasally with 10^4 PFU of MuHV-4 diluted in 30 μl of sterile PBS, under general anesthesia with isoflurane. For imaging, mice were injected intraperitoneally with luciferin (60 mg/kg of body weight) and imaged 10 min later with an IVIS Spectrum instrument (Caliper Life Sciences). For quantitative comparisons, we used Living Image software (Caliper Life Sciences) to obtain the average radiance (photons per second per square centimeter per steradian) over each region of interest. The background measured in the right abdominal region was removed from the measurements.

Viruses. All viruses were derived from a MuHV-4 bacterial artificial chromosome (BAC) (44). We used a mutant expressing firefly luciferase under the control of the M3 promoter (WT Luc$^+$) (8). The M7 sequence was disrupted via the insertion of an oligonucleotide containing stop codons in all reading frames and an EcoRI restriction site at an AfeI site (genomic position 69743; GenBank accession number AF105037.1) (20). We further mutated this virus to obtain gp150$^-$ Luc$^+$ MuHV-4 by the insertion of the luciferase coding sequence (8). Briefly, a luciferase coding sequence under the control of an M3 promoter and followed by a polyadenylation [poly(A)] signal was inserted into the MfeI site (genomic position 77176) between poly(A) signals of ORF57 and ORF58.

For *in vivo* experiments, the loxP-flanked BAC/enhanced green fluorescent protein (eGFP) cassette was removed by virus growth in NIH 3T3-CRE cells until eGFP$^+$ cells were no longer visible (45). Virus stocks were grown in BHK-21 cells cultured in Dulbecco's modified Eagle's medium (DMEM; Gibco) supplemented with 2 mM glutamine, 100 U penicillin ml^{-1}, 100 mg streptomycin ml^{-1}, and 10% fetal calf serum. Infected cells were cleared of cell debris by low-speed centrifugation (1,000 $\times$ *g* for 30 min). Viruses were then concentrated by high-speed centrifugation (58,000 $\times$ *g* for 90 min) and titrated by a plaque assay on BHK-21 cells (33).

Southern blotting. Viral DNA was digested with the EcoRI restriction enzyme, electrophoresed on a 0.8% agarose gel, and transferred to a positively charged nylon membrane. The membrane was hybridized with [^{32}P]dCTP-labeled probes and exposed to X-ray film.

Genome sequencing. Viral genomic DNA was extracted from purified virions, and full-length genome sequencing was performed as described previously (46).

Flow cytometry. Cells were infected with WT Luc$^+$ or gp150$^-$ Luc$^+$ MuHV-4 (1 PFU/cell) and incubated for 18 h. Cells were incubated with MuHV-4 glycoprotein-specific monoclonal antibodies

(MAbs) (4°C for 45 min). The MAbs used were MAb 3F7 (anti-gN) (14), MAb TIA1 (anti-gp150) (20), and MAb 8C1 (anti-gH) (47). Cells were then incubated with Alexa 633-conjugated goat anti-mouse polyclonal antibody (PAb) (Invitrogen) (4°C for 45 min). Cells were washed in PBS, and fluorescence was analyzed on a FACSAria cytometer (Becton Dickinson).

Infectious center assay. Reactivation of virus from the spleen was assayed by an infectious center assay (9). Briefly, 5×10^5 BHK-21 cells grown in 6-well cluster dishes were cocultured for 5 days at 37°C with an *ex vivo* spleen cell suspension in RPMI medium containing 2 mM glutamine, 100 U penicillin ml^{-1}, 100 mg streptomycin ml^{-1}, 10% fetal calf serum, 0.6% carboxymethyl cellulose (CMC), and 5×10^{-5} M β-mercaptoethanol. Cells were then fixed and stained for plaque counting.

Quantification of anti-MuHV-4-specific antibodies by an ELISA. Nunc MaxiSorp ELISA plates were coated for 18 h at 4°C with Triton X-100-disrupted MuHV-4 virions (10^6 PFU/well), blocked in PBS–0.1% Tween 20–3% bovine serum albumin (BSA), and incubated with mouse sera (diluted 1/200 in PBS–0.1% Tween 20) or with mouse vaginal fluids (50 μl/well). Bound antibodies were detected with alkaline phosphatase-conjugated goat anti-mouse Ig polyclonal antibody (Sigma). Washing was performed with PBS–0.1% Tween 20. *p*-Nitrophenylphosphate (Sigma) was used as the substrate for colorimetry, and the absorbance was read at 405 nm by using a Benchmark ELISA plate reader (Thermo).

Detection of infectious particles in vaginal fluids. Vaginal lavage fluids were obtained by gently flushing the mouse vagina with 200 μl of sterile PBS. Lavage fluids were successively centrifuged ($100 \times g$ for 10 min and $20{,}000 \times g$ for 1 h 30 min), and pellets from the two centrifugations were resuspended in 100 μl of sterile PBS. Samples were titrated on BHK-21 cells by a plaque assay.

Seroneutralization assay. Sera were collected from mice infected with either WT Luc^+ or $gp150^-$ MuHV-4 at 1 month postinfection. Virions were incubated with different dilutions of sera for 1 h at 37°C. The virus-serum mixtures were then added to 5×10^5 BHK-21 cells grown in 6-well cluster dishes, in complete DMEM with 0.6% CMC. Cells were cultured for 4 days before being fixed and stained for plaque counting.

Viral genome quantification. MuHV-4 genomic positions 40264 to 44385 were amplified (iCycler; Bio-Rad) (ORF25 forward primer 5′-ATGGTATAGCCGCCTTTGTG-3′ and reverse primer 5′-ACAAGTGGAT GAAGGGTTGC-3′). The PCR products were quantified by hybridization with a TaqMan probe (genomic positions 43088 to 43117 [5′-6-carboxyfluorescein {FAM}-TTCATAAGTTTTATGCTGATCCAGTGGTTG-black hole quencher 1 {BHQ1}-3′]) and converted to genome copy numbers by comparison with a standard curve of a cloned plasmid template serially diluted in control spleen DNA and amplified in parallel. Cellular DNA was quantified in parallel by amplifying part of the interstitial retinoid binding protein (IRBP) gene (forward primer 5′-ATCCCTATGTCATCTCCTACYTG-3′ and reverse primer 5′-CCRCTGCCTTCCCATG TYTG-3′). The PCR products were quantified with Sybr green (Invitrogen), and the copy number was calculated by comparison with standard curves of the cloned mouse IRBP template amplified in parallel. Amplified products were distinguished from paired primers by melting-curve analysis, and the correct sizes of the amplified products were confirmed by electrophoresis and staining with ethidium bromide.

Culture of vaginal epithelial cells. Vaginal tissues were dissected and incubated overnight at 4°C with 0.2% dispase II. Epithelial sheets were then separated from stroma, and the epithelium was cut into small pieces and incubated for 30 min in PBS–0.01% EDTA–0.025% trypsin. Cells were filtered on a 100-μm cell strainer and cultured on fibronectin-collagen precoated 24-well dishes (3×10^5 cells/well), as described previously (48). Cells were cultured 1/1 in Ham's F-12 medium–Dulbecco's modified Eagle's medium (Gibco) supplemented with 2 mM glutamine, 100 U penicillin ml^{-1}, 100 mg streptomycin ml^{-1}, 10% fetal calf serum, 2.5 μg amphotericin B ml^{-1}, 0.01 μg cholera toxin ml^{-1}, 10 μg insulin ml^{-1}, 10 μg transferrin ml^{-1}, 0.4 μg hydrocortisone ml^{-1}, 10 ng murine epidermal growth factor ml^{-1}, 50 μM beta-mercaptoethanol, and 20 μg adenine ml^{-1}.

Transmission electron microscopy. Samples were prepared for TEM as previously described (19). Briefly, cells were washed with PBS and fixed directly in the dish with cacodylate buffer containing 2.5% glutaraldehyde and 2% paraformaldehyde. The cells were then scraped off and prepared for electron microscopy. Epon blocks and sections were prepared as described previously (49). Sections were analyzed by using a Tecnai Spirit transmission electron microscope (FEI, Eindhoven, The Netherlands), and electron micrographs were taken by using a bottom-mounted 4K-by-4K-resolution Eagle camera (FEI).

ACKNOWLEDGMENTS

This work was supported by grant VIR-IMPRINT ARC from the University of Liège. C.Z. is a research fellow of the Fonds de la Recherche Scientifique-Fonds National Belge de la Recherche Scientifique (FRS-FNRS). The funders had no role in study design, data collection and interpretation, or the decision to submit the work for publication.

We thank L. Willems for helpful discussions and the technician and administrative team of the laboratory for very helpful assistance.

REFERENCES

1. Virgin HW, Wherry EJ, Ahmed R. 2009. Redefining chronic viral infection. Cell 138:30–50. https://doi.org/10.1016/j.cell.2009.06.036.
2. Henle G, Henle W, Clifford P, Diehl V, Kafuko GW, Kirya BG, Klein G, Morrow RH, Munube GM, Pike P, Tukei PM, Ziegler JL. 1969. Antibodies to Epstein-Barr virus in Burkitt's lymphoma and control groups. J Natl Cancer Inst 43:1147–1157.

3. Verma SC, Robertson ES. 2003. Molecular biology and pathogenesis of Kaposi sarcoma-associated herpesvirus. FEMS Microbiol Lett 222:155–163. https://doi.org/10.1016/S0378-1097(03)00261-1.
4. Davison AJ. 2011. Evolution of sexually transmitted and sexually transmissible human herpesviruses. Ann N Y Acad Sci 1230:E37–E49. https://doi.org/10.1111/j.1749-6632.2011.06358.x.
5. Schulz TF. 2000. Kaposi's sarcoma-associated herpesvirus (human herpesvirus 8): epidemiology and pathogenesis. J Antimicrob Chemother 45(Suppl T3):15–27. https://doi.org/10.1093/jac/45.suppl_4.15.
6. Dunmire SK, Grimm JM, Schmeling DO, Balfour HH, Jr, Hogquist KA. 2015. The incubation period of primary Epstein-Barr virus infection: viral dynamics and immunologic events. PLoS Pathog 11:e1005286. https://doi.org/10.1371/journal.ppat.1005286.
7. Barton E, Mandal P, Speck SH. 2011. Pathogenesis and host control of gammaherpesviruses: lessons from the mouse. Annu Rev Immunol 29:351–397. https://doi.org/10.1146/annurev-immunol-072710-081639.
8. Milho R, Smith CM, Marques S, Alenquer M, May JS, Gillet L, Gaspar M, Efstathiou S, Simas JP, Stevenson PG. 2009. In vivo imaging of murid herpesvirus-4 infection. J Gen Virol 90:21–32. https://doi.org/10.1099/vir.0.006569-0.
9. Francois S, Vidick S, Sarlet M, Desmecht D, Drion P, Stevenson PG, Vanderplasschen A, Gillet L. 2013. Illumination of murine gammaherpesvirus-68 cycle reveals a sexual transmission route from females to males in laboratory mice. PLoS Pathog 9:e1003292. https://doi.org/10.1371/journal.ppat.1003292.
10. Vidick S, Leroy B, Palmeira L, Machiels B, Mast J, Francois S, Wattiez R, Vanderplasschen A, Gillet L. 2013. Proteomic characterization of murid herpesvirus 4 extracellular virions. PLoS One 8:e83842. https://doi.org/10.1371/journal.pone.0083842.
11. Bortz E, Whitelegge JP, Jia Q, Zhou ZH, Stewart JP, Wu TT, Sun R. 2003. Identification of proteins associated with murine gammaherpesvirus 68 virions. J Virol 77:13425–13432. https://doi.org/10.1128/JVI.77.24.13425-13432.2003.
12. May JS, Coleman HM, Boname JM, Stevenson PG. 2005. Murine gammaherpesvirus-68 ORF28 encodes a non-essential virion glycoprotein. J Gen Virol 86:919–928. https://doi.org/10.1099/vir.0.80661-0.
13. May JS, de Lima BD, Colaco S, Stevenson PG. 2005. Intercellular gammaherpesvirus dissemination involves co-ordinated intracellular membrane protein transport. Traffic 6:780–793. https://doi.org/10.1111/j.1600-0854.2005.00316.x.
14. May JS, Colaco S, Stevenson PG. 2005. Glycoprotein M is an essential lytic replication protein of the murine gammaherpesvirus 68. J Virol 79:3459–3467. https://doi.org/10.1128/JVI.79.6.3459-3467.2005.
15. Gillet L, Adler H, Stevenson PG. 2007. Glycosaminoglycan interactions in murine gammaherpesvirus-68 infection. PLoS One 2:e347. https://doi.org/10.1371/journal.pone.0000347.
16. Gillet L, Colaco S, Stevenson PG. 2008. The murid herpesvirus-4 gH/gL binds to glycosaminoglycans. PLoS One 3:e1669. https://doi.org/10.1371/journal.pone.0001669.
17. Nemerow GR, Mold C, Schwend VK, Tollefson V, Cooper NR. 1987. Identification of gp350 as the viral glycoprotein mediating attachment of Epstein-Barr virus (EBV) to the EBV/C3d receptor of B cells: sequence homology of gp350 and C3 complement fragment C3d. J Virol 61:1416–1420.
18. Raab MS, Albrecht JC, Birkmann A, Yaguboglu S, Lang D, Fleckenstein B, Neipel F. 1998. The immunogenic glycoprotein gp35-37 of human herpesvirus 8 is encoded by open reading frame K8.1. J Virol 72:6725–6731.
19. Machiels B, Lete C, de Fays K, Mast J, Dewals B, Stevenson PG, Vanderplasschen A, Gillet L. 2011. The bovine herpesvirus 4 Bo10 gene encodes a nonessential viral envelope protein that regulates viral tropism through both positive and negative effects. J Virol 85:1011–1024. https://doi.org/10.1128/JVI.01092-10.
20. de Lima BD, May JS, Stevenson PG. 2004. Murine gammaherpesvirus 68 lacking gp150 shows defective virion release but establishes normal latency in vivo. J Virol 78:5103–5112. https://doi.org/10.1128/JVI.78.10.5103-5112.2004.
21. Gillet L, May JS, Stevenson PG. 2009. In vivo importance of heparan sulfate-binding glycoproteins for murid herpesvirus-4 infection. J Gen Virol 90:602–613. https://doi.org/10.1099/vir.0.005785-0.
22. Milho R, Frederico B, Efstathiou S, Stevenson PG. 2012. A heparan-dependent herpesvirus targets the olfactory neuroepithelium for host entry. PLoS Pathog 8:e1002986. https://doi.org/10.1371/journal.ppat.1002986.
23. Lawler C, Milho R, May JS, Stevenson PG. 2015. Rhadinovirus host entry by co-operative infection. PLoS Pathog 11:e1004761. https://doi.org/10.1371/journal.ppat.1004761.
24. Hayashi K, Hayashi M, Jalkanen M, Firestone JH, Trelstad RL, Bernfield M. 1987. Immunocytochemistry of cell surface heparan sulfate proteoglycan in mouse tissues. A light and electron microscopic study. J Histochem Cytochem 35:1079–1088. https://doi.org/10.1177/35.10.2957423.
25. Glauser DL, Kratz AS, Gillet L, Stevenson PG. 2011. A mechanistic basis for potent, glycoprotein B-directed gammaherpesvirus neutralization. J Gen Virol 92:2020–2033. https://doi.org/10.1099/vir.0.032177-0.
26. Glauser DL, Kratz AS, Stevenson PG. 2012. Herpesvirus glycoproteins undergo multiple antigenic changes before membrane fusion. PLoS One 7:e30152. https://doi.org/10.1371/journal.pone.0030152.
27. Subramanian R, Sehgal I, D'Auvergne O, Kousoulas KG. 2010. Kaposi's sarcoma-associated herpesvirus glycoproteins B and K8.1 regulate virion egress and synthesis of vascular endothelial growth factor and viral interleukin-6 in BCBL-1 cells. J Virol 84:1704–1714. https://doi.org/10.1128/JVI.01889-09.
28. Birkmann A, Mahr K, Ensser A, Yaguboglu S, Titgemeyer F, Fleckenstein B, Neipel F. 2001. Cell surface heparan sulfate is a receptor for human herpesvirus 8 and interacts with envelope glycoprotein K8.1. J Virol 75:11583–11593. https://doi.org/10.1128/JVI.75.23.11583-11593.2001.
29. Chesnokova LS, Valencia SM, Hutt-Fletcher LM. 2016. The BDLF3 gene product of Epstein-Barr virus, gp150, mediates non-productive binding to heparan sulfate on epithelial cells and only the binding domain of CD21 is required for infection. Virology 494:23–28. https://doi.org/10.1016/j.virol.2016.04.002.
30. Shannon-Lowe CD, Neuhierl B, Baldwin G, Rickinson AB, Delecluse HJ. 2006. Resting B cells as a transfer vehicle for Epstein-Barr virus infection of epithelial cells. Proc Natl Acad Sci U S A 103:7065–7070. https://doi.org/10.1073/pnas.0510512103.
31. Ruiss R, Ohno S, Steer B, Zeidler R, Adler H. 2012. Murine gammaherpesvirus 68 glycoprotein 150 does not contribute to latency amplification in vivo. Virol J 9:107. https://doi.org/10.1186/1743-422X-9-107.
32. Gillet L, Frederico B, Stevenson PG. 2015. Host entry by gammaherpesviruses—lessons from animal viruses? Curr Opin Virol 15:34–40. https://doi.org/10.1016/j.coviro.2015.07.007.
33. Gillet L, May JS, Colaco S, Stevenson PG. 2007. The murine gammaherpesvirus-68 gp150 acts as an immunogenic decoy to limit virion neutralization. PLoS One 2:e705. https://doi.org/10.1371/journal.pone.0000705.
34. Machiels B, Lete C, Guillaume A, Mast J, Stevenson PG, Vanderplasschen A, Gillet L. 2011. Antibody evasion by a gammaherpesvirus O-glycan shield. PLoS Pathog 7:e1002387. https://doi.org/10.1371/journal.ppat.1002387.
35. Stevenson PG, Doherty PC. 1998. Kinetic analysis of the specific host response to a murine gammaherpesvirus. J Virol 72:943–949.
36. Diehl WE, Lin AE, Grubaugh ND, Carvalho LM, Kim K, Kyawe PP, McCauley SM, Donnard E, Kucukural A, McDonel P, Schaffner SF, Garber M, Rambaut A, Andersen KG, Sabeti PC, Luban J. 2016. Ebola virus glycoprotein with increased infectivity dominated the 2013-2016 epidemic. Cell 167:1088.e6–1098.e6. https://doi.org/10.1016/j.cell.2016.10.014.
37. Shi Y, Wu Y, Zhang W, Qi J, Gao GF. 2014. Enabling the 'host jump': structural determinants of receptor-binding specificity in influenza A viruses. Nat Rev Microbiol 12:822–831. https://doi.org/10.1038/nrmicro3362.
38. Minor PD. 2000. Eradication of polio by vaccination. Virology 268:231–232. https://doi.org/10.1006/viro.2000.0208.
39. Bouma A. 2005. Determination of the effectiveness of pseudorabies marker vaccines in experiments and field trials. Biologicals 33:241–245. https://doi.org/10.1016/j.biologicals.2005.08.011.
40. Farrell HE, Lawler C, Tan CS, MacDonald K, Bruce K, Mach M, Davis-Poynter N, Stevenson PG. 2016. Murine cytomegalovirus exploits olfaction to enter new hosts. mBio 7:e00251-16. https://doi.org/10.1128/mBio.00251-16.
41. Hayashi K, Hayashi M, Boutin E, Cunha GR, Bernfield M, Trelstad RL. 1988. Hormonal modification of epithelial differentiation and expression of cell surface heparan sulfate proteoglycan in the mouse vaginal epithelium. An immunohistochemical and electron microscopic study. Lab Invest 58:68–76.
42. Turk SM, Jiang R, Chesnokova LS, Hutt-Fletcher LM. 2006. Antibodies to gp350/220 enhance the ability of Epstein-Barr virus to infect epithelial cells. J Virol 80:9628–9633. https://doi.org/10.1128/JVI.00622-06.
43. Gillet L, May JS, Stevenson PG. 2007. Post-exposure vaccination improves gammaherpesvirus neutralization. PLoS One 2:e899. https://doi.org/10.1371/journal.pone.0000899.
44. Adler H, Messerle M, Wagner M, Koszinowski UH. 2000. Cloning and mutagenesis of the murine gammaherpesvirus 68 genome as an infec-

tious bacterial artificial chromosome. J Virol 74:6964–6974. https://doi.org/10.1128/JVI.74.15.6964-6974.2000.
45. Adler H, Messerle M, Koszinowski UH. 2001. Virus reconstituted from infectious bacterial artificial chromosome (BAC)-cloned murine gammaherpesvirus 68 acquires wild-type properties in vivo only after excision of BAC vector sequences. J Virol 75:5692–5696. https://doi.org/10.1128/JVI.75.12.5692-5696.2001.
46. Latif MB, Machiels B, Xiao X, Mast J, Vanderplasschen A, Gillet L. 2016. Deletion of murid herpesvirus 4 ORF63 affects the trafficking of incoming capsids toward the nucleus. J Virol 90:2455–2472. https://doi.org/10.1128/JVI.02942-15.
47. Gill MB, Gillet L, Colaco S, May JS, de Lima BD, Stevenson PG. 2006. Murine gammaherpesvirus-68 glycoprotein H-glycoprotein L complex is a major target for neutralizing monoclonal antibodies. J Gen Virol 87:1465–1475. https://doi.org/10.1099/vir.0.81760-0.
48. Hakkinen L, Koivisto L, Larjava H. 2001. An improved method for culture of epidermal keratinocytes from newborn mouse skin. Methods Cell Sci 23:189–196. https://doi.org/10.1023/A:1016385109922.
49. Mast J, Nanbru C, van den Berg T, Meulemans G. 2005. Ultrastructural changes of the tracheal epithelium after vaccination of day-old chickens with the La Sota strain of Newcastle disease virus. Vet Pathol 42:559–565. https://doi.org/10.1354/vp.42-5-559.